

Temperature Distribution and Its Influence on the Growth of Titania/Zirconia Nanotubes During Anodization

Jianling Zhao¹, Xixin Wang^{1,*}, Xiaohui Wang², Ji Zhou²

¹ School of Material Science and Engineering, Hebei University of Technology, Tianjin 300130, PR China

² Department of Materials Science and Engineering, Tsinghua University, Beijing 100084, PR China

*E-mail: zhaojl02@126.com; xixinwang@126.com

Received: 13 July 2012 / *Accepted:* 26 September 2012 / *Published:* 1 November 2012

Titania and zirconia nanotubes were prepared in aqueous and organic electrolytes through anodization method. The bottom morphology and oxide composition were investigated via transmission electron microscopy and Fourier transform infrared spectroscopy. Influences of mass transfer, heat transfer and electrolyte properties on the growth of nanotubes have been discussed in detail. During anodization, inhomogeneous mass transfer and heat transfer result in inhomogeneous temperature distribution and different oxide compositions between the bottom and wall of nanotubes. On the one hand, the tube wall with lower hydroxyl content is more difficult to be dissolved than the tube bottom with higher hydroxyl content. On the other hand, the higher temperature at tube bottom results in stronger oxide dissolution than that at the tube wall. All these effects lead to the longitudinal growth of the nanotubes during anodization process because the dissolution rate at tube bottom is larger than that at tube wall.

Keywords: nanotubes; anodization; temperature distribution; growth mechanism

1. INTRODUCTION

Metal oxide nanochannel structures including alumina nanopore arrays [1], titania nanotube arrays [2-4], zirconia nanotube arrays [5, 6], and so forth have been successfully fabricated by the anodization method [7-12] in recent years. The nanochannel structure may improve and enhance the performance of metal oxides and have vast application prospects [13, 14]. For example, titania nanotube arrays and zirconia nanotube arrays have outstanding properties in photocatalysis [15], water decomposition [16], solar energy cell [17, 18], catalyst [19-21], gas sensitivity [22-24], photoelectroactivity [25], biological activity [26, 27], dye degradation [28], and so forth.

A widely accepted nanotube growth mechanism is the dissolution action under electric field induction [29-33]. Obviously, the larger difference in dissolution between tube bottom and tube wall are favorable to longitudinal growth of the nanotubes during anodization process. Previous studies show that titania and zirconia nanotubes with a length more than 100 μm have been prepared in organic electrolytes (e.g. ethylene glycol, dimethyl sulfoxide (DMSO), N-methyl formamide (NMF), formamide (FA), glycerol, etc.) [34-38]. Preparation of nanotubes longer than 100 μm indicates that the tube wall which is generally a few to a few tens of nanometers in thickness has poor dissolution while the tube bottom has better dissolution in organic electrolytes. The great difference in dissolution between the wall and bottom cannot be explained completely and satisfactorily only through field-assistant dissolution phenomenon. In this paper, from the viewpoint of mass transfer and heat transfer, the reasons why there are so great dissolution difference between tube wall and bottom have been discussed in detail via investigations of preparation of titania and zirconia nanotubes by anodization process. Influences of electrolytes on the nanotube growth process have also been discussed.

2. EXPERIMENTAL

The metal foils (Ti or Zr, 99.7% purity, $10 \times 10 \times 0.5 \text{ mm}^3$) used in this study were obtained from the General Research Institute for Nonferrous Metals (Beijing, China). They were polished mechanically and washed in twice-distilled water and acetone by ultrasonic washing before use. Ti or Zr foils were anodized using a program-controlled DC source (Dahua Coop., Beijing, China) in different kinds of electrolyte and the electrode distance was kept at 2 cm. During the experiments, the electrolyte solutions were stirred using a magnetic stirrer. After anodization, the samples were rinsed in deionized water, dried and characterized through transmission electron microscopy (TEM-200CX, JEOL, Japan) and Fourier transform infrared spectroscopy (FTIR, WQF-410, China).

3. RESULTS AND DISCUSSION

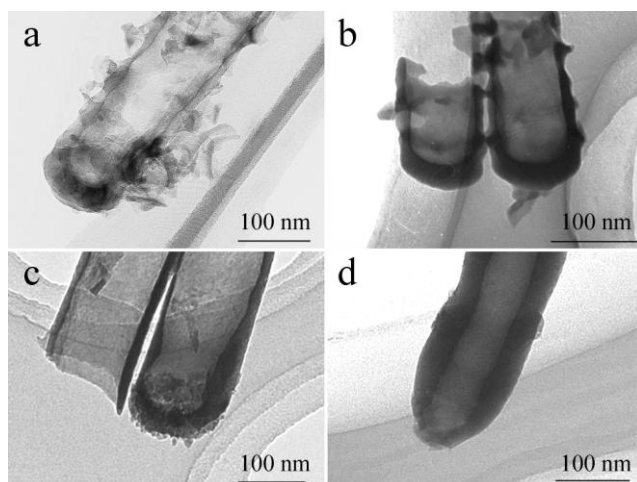


Figure 1. Bottom TEM images of titania and zirconia nanotubes: (a) Ti, 1M H_3PO_4 +0.5% $\text{HF}+\text{H}_2\text{O}$, 20V, 1h; (b) Ti, 1% $\text{HF}+\text{H}_2\text{O}$, 20V, 30min; (c) Zr, formamide and glycerol (volume ratio=1:1) + 2 wt% HCl + 3.5 wt% H_2O 20V, 5h; (d) Zr, formamide and glycerol (volume ratio=1:1) +1% NH_4F +3% H_2O , 50V, 24h

Figure 1 shows the bottom TEM images of titania and zirconia nanotubes prepared in different electrolytes. The color of the bottom and wall of titania nanotubes prepared in aqueous solution is similar and the thickness of tube bottom is obviously larger than that of the tube wall (Fig.1a, b). The bottom of zirconia nanotubes prepared in mixture of formamide and glycerol (volume ratio=1:1) containing 2 wt% HCl and 3.5 wt% H₂O is loose (Fig.1c) and the bottom color of zirconia nanotubes prepared in mixture of formamide and glycerol (volume ratio=1:1) containing 1wt% NH₄F and 3wt% H₂O is obviously lighter than that of the tube wall (resembling gelatin) (Fig.1d). Figure 1 shows that the electrolytes have great impact on the morphology of nanotube bottom.

FTIR spectra of titania nanotubes annealed at different temperatures are shown in Figure 2. The peaks at 3430 and 1630 cm⁻¹ can be assigned to the absorption of water. The peaks at 3026, 2925, 2850, 1493, 1452, 1398, 756, 698 cm⁻¹ correspond to the characteristic absorption of titania. The intensity of the Ti-OH absorption peak at 1398 cm⁻¹ decreases with the increasing annealed temperature, which is identical to the FTIR results of zirconia nanotubes [38]. The FTIR spectra analysis show that titania and zirconia nanotubes prepared through anodization method contain many hydroxyl groups and the hydroxyl amount decreases with the increasing annealed temperature. The results are concordant with references [39-42].

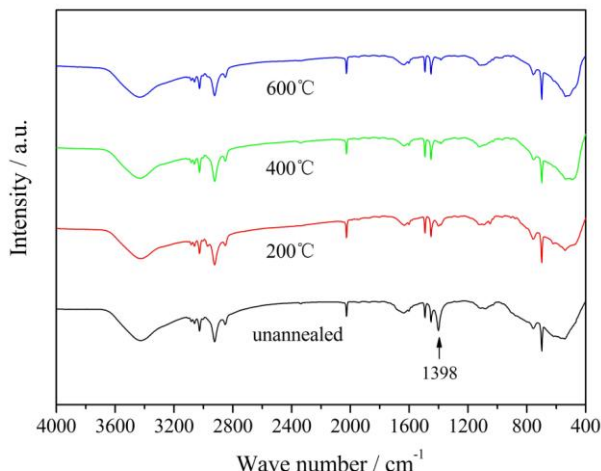
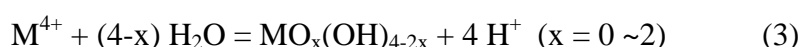
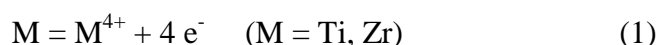


Figure 2. FTIR spectra of titania nanotubes annealed at different temperatures

Therefore, the anodization product of Ti and Zr can be represented with MO_x(OH)_{4-2x} (x = 0 ~2) and the anodization reactions can be shown as Equation 1 ~3.



Metal (M) loses electrons to form metal ions M^{4+} (Equation 1) and then metal ions react with X^- or H_2O in the electrolytes (Equation 2 and 3). Equation 2 results in the formation of $[MX_6]^{2-}$ and dissolution in the electrolytes and Equation 3 leads to the formation of oxides on the metal surface. The amount of metal ions formed in Equation 1 is definite. Consequently, when the reaction rate of Equation 2 increases, the reaction rate of Equation 3 would decrease correspondingly, and vice versa.

After the formation of nanotubes, mass transfer would affect the reaction rates of Equation 2 and 3 at tube bottom. The driving force of mass transfer comes from the action of the electric field on charged ions and the concentration gradient of the solution constituents, the action of electric field playing a predominant role.

When anodization is conducted in organic electrolytes containing a low amount of water, mass transfer affects the reaction rate of Equation 3 much apparently. Due to the blockage effects of the tube wall, mass transfer at the center area of tube axis is larger than that at the tube wall [43]. Therefore, there are much more X^- at the center part of the tube bottom than that at the tube wall, which results in the faster reaction rate of Equation 2 and the relatively slower reaction rate of Equation 3. Consequently, less few oxides form at the tube bottom than that of the tube wall. When anodization is conducted in aqueous solution, similar amount of oxides would form at the reaction interface because there is sufficient water and mass transfer hardly affects the reaction rate of Equation 3.

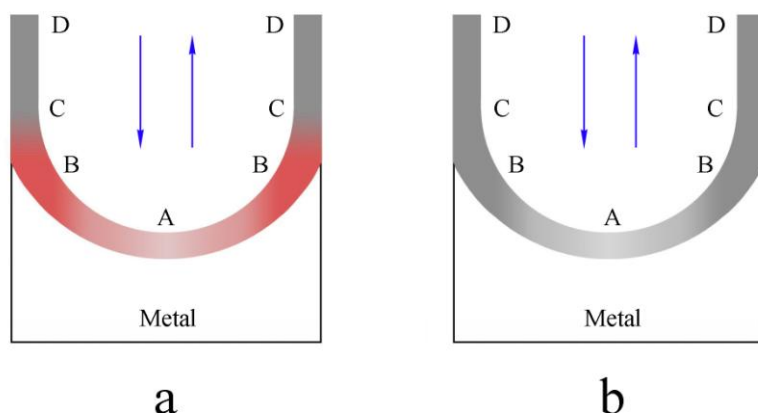


Figure 3. Influence of temperature on the oxide composition: (a) temperature distribution (dark red: higher temperature; light red: lower temperature); (b) oxide composition (dark grey: lower hydroxyl content; light grey: higher hydroxyl content)

A large amount of heat which is liberated during anodization of Ti and Zr ($\Delta H_{Ti} = -944 \text{ kJ}\cdot\text{mol}^{-1}$, $\Delta H_{Zr} = -1101 \text{ kJ}\cdot\text{mol}^{-1}$, [44]) would result in the temperature increase at the reaction interface (the tube bottom). The heat would be transferred outward through heat transfer which results in the temperature decrease at the reaction interface (the tube bottom). Mass transfer velocity affects heat transfer ability of the electrolytes, higher mass transfer velocity results in better heat transfer ability and lower reaction interface temperature at the tube bottom. The mass transfer velocity in the center area of the tube bottom is larger than that at the tube wall, resulting in the inhomogeneous temperature distribution in the tube bottom [43]. As shown in Fig.3a, from point A to point B the temperature

would increase. From point B to C, because there are less heat liberated at the interface, the temperature would decrease gradually and be close to the electrolyte temperature at point C. From point C to point D, the temperature is same as the electrolyte temperature. The temperature distribution can be described as: $T_B \geq T_A \geq T_C = T_D$.

The thermal conductivity of electrolytes also affects the temperature distribution at the tube bottom. The thermal conductivity of frequently-used solvents is listed in Table 1. The organic electrolytes with lower thermal conductivity have lower heat transfer velocity and lead to higher temperature at the tube bottom ($T_B > T_A > T_C = T_D$). As discussed in the above-mentioned FTIR spectra, temperature affects the hydroxyl content of the oxides according to Equation 3. In Fig.3a, from point A to point B, temperature increases gradually and hydroxyl contents of the oxides decrease gradually. As shown in Fig.3b, during anodization, along with downward movement of the reaction interface, the oxides at point B are partly dissolved in the electrolytes, the undissolved remnants constitute the tube wall. Therefore, when anodization is conducted in organic electrolytes, the hydroxyl contents of the tube wall are lower than that of the tube bottom.

The thermal conductivity of water is 2-3 times larger than that of the organic electrolytes. When anodization is conducted in aqueous solutions, fast heat transfer velocity results in a relatively homogeneous temperature distribution ($T_B \approx T_A \approx T_C = T_D$) and similar oxide composition of the tube wall with that of the tube bottom.

Table 1. Thermal conductivity of frequently-used solvents

Substance	Formula	Thermal Conductivity [44] (mJ·cm ⁻¹ ·s ⁻¹ ·K ⁻¹ , 298K)
Dimethyl sulfoxide	(CH ₃) ₂ SO	1.96 [45]
N-Methylformamide	HCONHCH ₃	2.03
Formamide	HCONH ₂	3.51 [46]
1, 2-Ethanediol	HOCH ₂ CH ₂ OH	2.56
Glycerol	HOCH ₂ CH(OH)CH ₂ OH	2.92
Water	H ₂ O	6.07

During anodization, the oxides would be dissolved in the electrolytes (Equation 4). Dissolution in aqueous solution is much easier than that in organic electrolytes. Dissolution of oxides would be affected by temperature, mass transfer velocity and the oxide composition, etc. Higher temperature and faster mass transfer velocity would accelerate the dissolution of oxides. Under the same conditions, oxides formed at higher temperature have lower hydroxyl contents and would be dissolved in the electrolytes difficultly [47, 48].



According to the above analysis, when anodization is conducted in organic electrolytes, faster mass transfer velocity, higher temperature and higher hydroxyl contents of oxides (Fig.3a, point A)

would result in the easy dissolution of the oxides at tube bottom. Mass transfer velocity and hydroxyl contents of oxides decrease from point A to point B, however, the temperature increases slightly, therefore, the oxides can still be dissolved in the electrolytes. From point B to point C, the oxide composition does not change, however, mass transfer velocity and temperature decrease gradually, therefore, oxides would be more difficult to be dissolved in electrolytes. From point C to point D, oxides are hardly soluble.

In brief, due to the influence of mass transfer and heat transfer, the inhomogeneous distribution of oxides composition and dissolution would lead to the increasing length of nanotubes and the appearance of bottom morphology in Fig.1c,d at the tube bottom in organic electrolytes.

When anodization is conducted in aqueous solutions, mass transfer and heat transfer have very little effect. The similar temperature and hydroxyl content of oxides together with the strong dissolution ability of aqueous solution lead to little dissolution difference. Dissolution takes place at both inside and outside of the tube wall [49]. As for the tube bottom, the side near the electrolytes would be dissolved and the side near the metal would form new oxides. These factors lead to the bottom morphology as shown in Fig.1a,b.

4. CONCLUSIONS

During anodization, the inhomogeneous mass transfer and heat transfer result in the inhomogeneous temperature distribution and different oxide compositions between the tube wall and bottom. On the one hand, the hydroxyl contents of the oxides are lower and the oxides are difficult to be dissolved at tube wall than that at tube bottom. On the other hand, the temperature is higher and the oxides are easy to be dissolved at the tube bottom than that at tube wall. Under the joint action of both effects, the oxides would dissolve much faster at tube bottom than that at tube wall and lead to the longitudinal growth of the nanotubes.

When anodization is conducted in organic electrolytes, the oxides at tube wall is difficult (or hardly) to be dissolved while the oxides at tube bottom is easy to be dissolved in the electrolytes because of the lower thermal conductivity and the weaker dissolution ability of the electrolytes, as well as the larger difference of temperature and hydroxyl content of the oxides. In aqueous solution, stronger dissolution ability and larger thermal conductivity of the electrolytes, as well as the similar temperature and hydroxyl content of oxides between tube bottom and wall are unfavorable to the growth of nanotubes. Consequently, longer nanotubes are easy to be prepared in organic electrolytes.

ACKNOWLEDGMENTS

This work is supported by National Natural Science Foundation of China (No. 50972036 and 51272064), Support Program for Hundred Excellent Innovation Talents from the Universities and Colleges of Hebei Province and Key Basic Research Program of Hebei Province of China (No. 12965135D).

References

1. H. Masuda, K. Fukuda, *Science*, 268 (1995) 1466
2. J.M. Macak, H. Tsuchiya, L. Taveira, S. Aldabergerova, P. Schmuki, *Angewandte Chemie International Edition*, 44 (2005) 7463
3. J. Zhao, X. Wang, T. Sun, L. Li, *Nanotechnol.* 16 (2005) 2450
4. J. Tao, J. Zhao, X. Wang, Y. Kang, Y. Li, *Electrochim. Commun.*, 10 (2008) 1161
5. H. Tsuchiya, J.M. Macak, L. Taveira, P. Schmuki, *Chem. Phys. Lett.*, 410 (2005) 188
6. J. Zhao, R. Xu, X. Wang, Y. Li, *Corrosion Science*, 50 (2008) 1593
7. H.E. Prakasam, O.K. Varghese, M. Paulose, G.K. Mor, C.A. Grimes, *Nanotechnol.*, 17 (2006) 4285
8. J. Choi, J.H. Lim, J. Lee, K.J. Kim, *Nanotechnol.*, 18 (2007) 055603
9. W. Wei, J. Macak, P. Schmuki, *Electrochim. Commun.*, 10 (2008) 428
10. S. Berger, H. Tsuchiya, A. Ghicov, P. Schmuki, *Appl. Phys. Lett.*s, 88 (2006) 203119
11. H.C. Shin, J. Dong, M. Liu, *Adv. Mater.*, 16 (2004) 237
12. W. Wei, H. Jha, G. Yang, R. Hahn, I. Paramasivam, S. Berger, E. Spiecker, P. Schmuki, *Adv. Mater.*, 22 (2010) 4770
13. G. Shen, P.C. Chen, K. Ryu, C. Zhou, *J. Mater. Chem.*, 19 (2009) 828
14. P. Roy, S. Berger, P. Schmuki, *Angewandte Chemie International Edition*, 50 (2011) 2904
15. C. Ruan, M. Paulose, O.K. Varghese, C.A. Grimes, *Solar energy materials and solar cells*, 90 (2006) 1283
16. J.H. Park, S. Kim, A.J. Bard, *Nano letters*, 6 (2006) 24
17. G.K. Mor, K. Shankar, M. Paulose, O.K. Varghese, C.A. Grimes, *Nano letters*, 6 (2006) 215
18. J. Zhao, X. Wang, Y. Kang, X. Xu, Y. Li, *Photonics Technol. Lett., IEEE*, 20 (2008) 1213
19. J. Macak, P. Barczuk, H. Tsuchiya, M. Nowakowska, A. Ghicov, M. Chojak, S. Bauer, S. Virtanen, P. Kulesza, P. Schmuki, *Electrochim. Commun.*, 7 (2005) 1417
20. X. Wang, J. Zhao, X. Hou, Q. He, C. Tang, *J. Nanomater.*, 2012 (2012) 1
21. X. Wang, J. Zhao, X. Hou, F. Wang, C. Tang, *Reaction Kinetics, Mechanisms and Catalysis*, 104 (2011) 227
22. M. Paulose, O.K. Varghese, G.K. Mor, C.A. Grimes, K.G. Ong, *Nanotechnol.*, 17 (2006) 398
23. S. Lin, D. Li, J. Wu, X. Li, S. Akbar, *Sensors and Actuators B: Chemical*, (2011) 505
24. H.F. Lu, F. Li, G. Liu, Z.G. Chen, D.W. Wang, H.T. Fang, G.Q. Lu, Z.H. Jiang, H.M. Cheng, *Nanotechnology*, 19 (2008) 405504
25. K. Raja, M. Misra, V. Mahajan, T. Gandhi, P. Pillai, S. Mohapatra, *J. Power Sources*, 161 (2006) 1450
26. L. Guo, J. Zhao, X. Wang, R. Xu, Z. Lu, Y. Li, *Mater. Sci. Engin.: C*, 29 (2009) 1174
27. L. Guo, J. Zhao, X. Wang, X. Xu, H. Liu, Y. Li, *Int. J. Appl. Ceramic Technol.*, 6 (2009) 636
28. J. Zhao, X. Wang, L. Zhang, X. Hou, Y. Li, C. Tang, *J. Hazard. Mater.* (2011)
29. G. Singh, A. Golovin, I. Aranson, *Physical Review B*, 73 (2006) 205422
30. Q. Huang, W. Lye, M. Reed, *Nanotechnol.*, 18 (2007) 405302
31. K. Yasuda, J.M. Macak, S. Berger, A. Ghicov, P. Schmuki, *J. Electrochem. Soc.*, 154 (2007) C472
32. J. Zhao, X. Wang, R. Chen, L. Li, *Solid state commun.*, 134 (2005) 705
33. J. Tao, J. Zhao, C. Tang, Y. Kang, Y. Li, *New J. Chem.*, 32 (2008) 2164
34. M. Paulose, H.E. Prakasam, O.K. Varghese, L. Peng, K.C. Popat, G.K. Mor, T.A. Desai, C.A. Grimes, *J. Phys. Chem. C*, 111 (2007) 14992
35. S.P. Albu, A. Ghicov, J.M. Macak, P. Schmuki, *physica status solidi (RRL)-Rapid Research Letters*, 1 (2007) R65
36. M. Paulose, K. Shankar, S. Yoriya, H.E. Prakasam, O.K. Varghese, G.K. Mor, T.A. Latempa, A. Fitzgerald, C.A. Grimes, *J. Phys. Chem. B*, 110 (2006) 16179

37. K. Shankar, G.K. Mor, H.E. Prakasam, S. Yoriya, M. Paulose, O.K. Varghese, C.A. Grimes, *Nanotechnology*, 18 (2007) 065707
38. J. Zhao, X. Wang, R. Xu, F. Meng, L. Guo, Y. Li, *Mater. Lett.*, 62 (2008) 4428
39. F.M. Bayoumi, B.G. Ateya, *Electrochim. Commun.*, 8 (2006) 38
40. D. Peng, X. Bai, X. Chen, Q. Zhou, X. Liu, R. Yu, *Appl. Surf. Sci.*, 221 (2004) 259
41. Y.T. Sul, C.B. Johansson, Y. Jeong, T. Albrektsson, *Medical engineering & physics*, 23 (2001) 329
42. A. Kanta, R. Sedev, J. Ralston, *Langmuir*, 21 (2005) 2400
43. X. Wang, J. Zhao, X. Wang, J. Zhou, *ISRN Nanotechnology*, 2011 (2011) 480970
44. J.G. Speight, Lange's handbook of chemistry, McGraw-Hill New York, 2005.
45. C. Nieto-Draghi, J.B. Ávalos, B. Rousseau, *J. Phys. Chem.*, 119 (2003) 4782
46. Y.A. Ganiev, Y.L. Rastorguev, *Journal of Engineering Physics and Thermophysics*, 15 (1968) 880
47. X. B, Application of zirconium, hafnium and their compounds Metallurgical Industry Press, 2002.
48. Z. Tang, in, Beijing: Chemical Industry Press, 2000.
49. K. Yasuda, P. Schmuki, *Electrochimica acta*, 52 (2007) 4053